http://journal.uir.ac.id/index.php/JGEET

E-ISSN : 2541-5794
P-ISSN : 2503-216X

Journal of Geoscience,
Engineering, Environment, and Technology
Vol 9 No 3 2024

RESEARCH ARTICLE

Coulomb Stress Change of Active Fault in South Sumatra Region Revealed from Kerinci Earthquake October 06, 1995 Mw 6.7 and Sungai Penuh Earthquake October 01, 2009 Mw 6.6

Rafi Fadhlurrohman[1], S. Syafriani[1*], Furqon D. Raharjo[1,2], Yusran Asnawi[3], Suaidi Ahadi[2]

[1]*Department of Physics, Universitas Negeri Padang, Padang 25131, Indonesia*
[2] *Indonesian Meteorology, Climatology, and Geophysics Agency, Indonesia*
[3]*Department of Science, Universitas Islam Negri Ar-Raniry, Aceh 23126, Indonesia*

* Corresponding author : syafri@fmipa.unp.ac.id
Received: Oct 1, 2016; Accepted: Nov 20, 2016.
DOI: 10.25299/jgeet.2024.9.3.19273

Abstract

We successfully highlight the correlation of Static Stress Change (ΔCFF) in the Kerimci earthquake October 06, 1995 Mw 6.7 and Sungai Penuh earthquake October 01, 2009 Mw 6.6 earthquakes to the seismicity conditions. The data used in this study are focal mechanism obtained from Global Centroid Moment Tensor (GCMT) and seismicity obtained from USGS with M ≥ 4 after the main earthquake with a time span of 11 years. ΔCFF obtained in the Mentawai Fault System area has increased coulomb stress. ΔCFF obtained in the Suliti Segment, Ketaun Segment, and Back arc Basin of Jambi experienced an increase in stress, which can indicate the potential for future earthquakes, but there was no increase in seismicity. Besides that, ΔCFF in areas that experienced a decrease in stress, experienced an increase in seismicity. This is caused by background seismicity in the area and several factors influence the results of the calculation of ΔCFF against seismicity. Simplicity in calculation causes difficulty in explaining seismicity, especially in the blue lobe. Moreover, the use of receiver fault mechanism produces a very large error in the complex regional stress field. The use of a constant friction coefficient also produces a very large error in the calculation.

Keywords: Static Coulomb stress, Background Seismicity, Province Jambi Surrounds

1. Introduction

The subduction activity of the Indo-Australian Plate, which moves obliquely with a relative velocity of 44 - 68 mm/year (DeMets et al., 2010), subducting the Euresian Plate with a dip angle of ~40° (Weller et al., 2012) causes the formation of the Sumatra Fault Sytem. This fault has a length of ± 1900 kilometers which is divided into 19 major faults (Sieh & Natawidjaja, 2000) as shown in Figure 1. These faults are spread along Sumatra Island from Lampung to Banda Aceh. The Sumatra Fault System is categorized as relatively active with right lateral - strike slip activity (Genrich et al., 2000) with a movement of 15 mm/year in each area it passes through (Natawidjaja, 2018). More than 20 damaging earthquakes of magnitude more than six have been recorded along this fault in the last 100 years (Bellier et al., 1997, Pasari et al., 2021).

On October 6, 1995 at 1:18 a.m. an earthquake with a magnitude of 6.7 occurred. According to the Global CMT (GCMT) (https://www.globalcmt.org/), the earthquake was located at 1.93 N and 101.31 E with a depth of 16.7 km. The earthquake caused 84 deaths, 558 serious injuries and 1,310 minor injuries. Meanwhile, 7,137 houses, transportation facilities, irrigation facilities, places of worship, markets and shops were damaged. In addition, on October 10, 2009 at 08:50 a.m. an earthquake with Mw 6.6 occurred. This earthquake was located at 2.45° N and 101.59° E with a depth of 15.1 km. This earthquake caused 1,100 houses to suffer heavy and light damage (Figure 2). Based on the location of the earthquakes (Figures 2), both earthquakes were located on the Sumatra fault system. The 1995 Mw 6.7 earthquake was occurred in the Siulak segment of Kerinci Regency and felt strongly by local peoples.

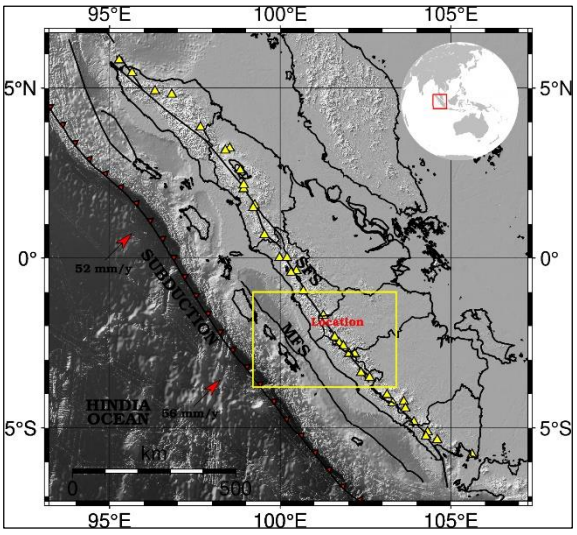

Fig. 1. The tectonic map shows the fault system in the Sumatra Island where the subduction zone in the western part and the Sumatra fault in the land. The yellow triangles depict the volcanic system in the Sumatra Island. The red square is the study area of this research.

This segment stretches from -1.7o N to 2.25o N and extends from the northwest to the southern boundary of Lake Kerinci and continues to the memping river. The

segment is 70 km long and about 11 km wide. In addition, the northern part of this segment contains an active volcano, Mount Kerinci.The 2009 Mw 6.6 earthquake was located in the dikit segment, sungai penuh city. This segment stretches from 2.3° LS - 2.75° LS with a fault length of about 60 km. The fault extends from Gunung Pandan along the Langkup River to Gunung Kunyit. In the eastern part of this segment, there are 3 volcanic mountains that extend about two-thirds of the segment (Salman et al., 2020, Nurana et al., 2021). Triggering seismicity activity by large earthquakes is a phenomenon that occurs everywhere. Seismicity study is one of the ways to study the influence of one earthquake to another and the easiest way to see the seismicity behavior of the region because it is directly related to the mainshock (e. g. Kilb et al., 2002, Simanjuntak & Olymphia, 2017, Asnawi et al., 2020, Pasari et al., 2021, Simanjuntak & Ansari, 2022). The change and direction of seismicity after a large earthquake remains a question until now. One method that can be used to look at seismicity activity is by looking at the correlation between coulomb failure stress (ΔCFF) and seismicity after an earthquake.

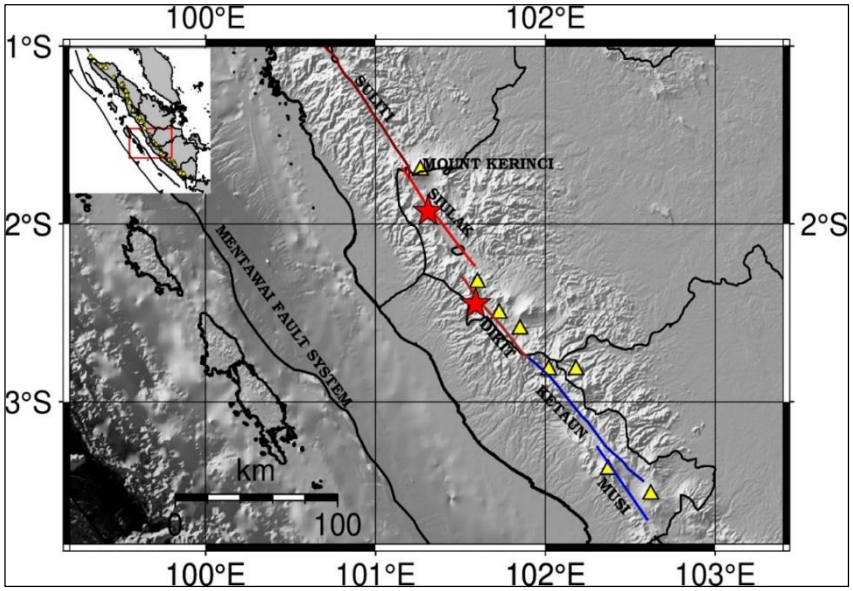

Fig. 3. Tectonic conditions of Jambi Province and surroundings. The red star is the epicenter of the earthquakes according to Global CMT.

The triggering of earthquakes and the increase in seismicity by large earthquakes have been investigated using static changes in coulomb failure stress (ΔCFF) by (Harris & Simpson, 1996; Parsons & Dreger, 2000; Stein et al., 1992, 1994; Toda et al., 1998, Qadariyah et al., 2018, Simanjuntak & Ansari, 2023, Simanjuntak & Ansar, 2024, Adi et al., 2024, Ansari et al., 2024). In this paper, we will try to understand and explain the influence of tectonic coulomb stress on seismic conditions in the study area. According to the coulomb stress theory, areas that experience increased coulomb stress have the potential for earthquakes to occur.

2. Data and Methods

We use data from USGS with M ≥ 4 for seismicity (https://earthquake.usgs.gov/earthquakes/search/) after the earthquake with a time span of 11 years. We use Global CMT (GCMT) using 2 Nodal Planes for calculate Static Coulomb Stress. Then, the parameters to be used are moment tensor (strike, dip, rake), epicenter (longitude, latitude), hypocenter (depth) and magnitude. After that, calculating the rupture area based on the empirical relationship of the (Wells & Coppersmith, 1994). After that, the calculation of coulomb failure stress (ΔCFF) is carried out to see the triggering of earthquake and seismic activity (Toda & Stein, 2002 , Simanjuntak et al., 2024) as shown in Equation (1).

$$\Delta CFF = \Delta\tau + \mu'\Delta\sigma \quad (1)$$

where τ is the shear stress, σ is the normal stress, and μ' is the effective coefficient dimana μ' yang digunakan adalah μ'=0.4 (Charles et al., 1994). The calculation of earthquake triggering ΔCFF in this study uses receiver fault with specified oriented (Toda, 2008; Woessner et al., 2012) where in this study using the mainshcock mechanism, namely the calculation of depth based on the center of the fault plane.

We use shear modulus of 3.2 x 10^5 bars and Poisson's ratio of 0.25 with the assumption that the earth is considered as a homogeneous elastic half space and fault as rectangular dislocations embedded within it (Lin & Stein, 2004; Okada, 1992, Asnawi et al., 2022). In principle, if ΔCFF > 0, then this area is an area that experiences increased stress so that there is an increase in seismicity in the area. Whereas ΔCFF < 0, is an area that experiences a decrease in stress so that it experiences a decrease in seismicity.

3. Results and Discussion

Based on the parameters obtained from GCMT, there are 2 nodal planes as shown in Table 1. Based on the parameters above, mapping was done to see the focal mechanism of the earthquake as shown Figure 3. Based on Figure 3, it can be seen that both earthquakes were Strike - Slip earthquakes. This is in accordance with the movement of the Sumatra Fault System, which is Strike - slip. Then the coulomb stress measurement was carried out using equation 1.

Table 1. Parameters in coulomb stress processing. Longitude, latitude, depth, moment tensor (strike, dip, and rake), Magnitude. Then calculate the rupture area (length and width) (based on empirical relationship of (Wells & Coppersmith, 1994).

Location	Lat (°)	Long (°)	Nodal Plane	Strike (°)	Dip (°)	Rake (°)	Depth (km)	Mw	Length (km)	Width (km)	Fm
Kerinci	-1.93	101.31	NP 1 NP 2	326 235	74 87	-177 -16	16.7	6.7	38.96	13.17	
Sungai Penuh	-2.45	101.59	NP 1 NP 2	323 232	70 88	-178 -20	15.1	6.6	33.38	12.05	

This is in accordance with the movement of the Sumatra Fault System, which is Strike - slip. Then the coulomb stress measurement was carried out using equation 1. In this processing, 2 Nodal Planes are used and seismicity after the earthquake is depicted with a time span of 11 years. Processing coulomb stress change Kerinci earthquake October 6, 1995 with Nodal Plane 1 can be seen in Figures 4.

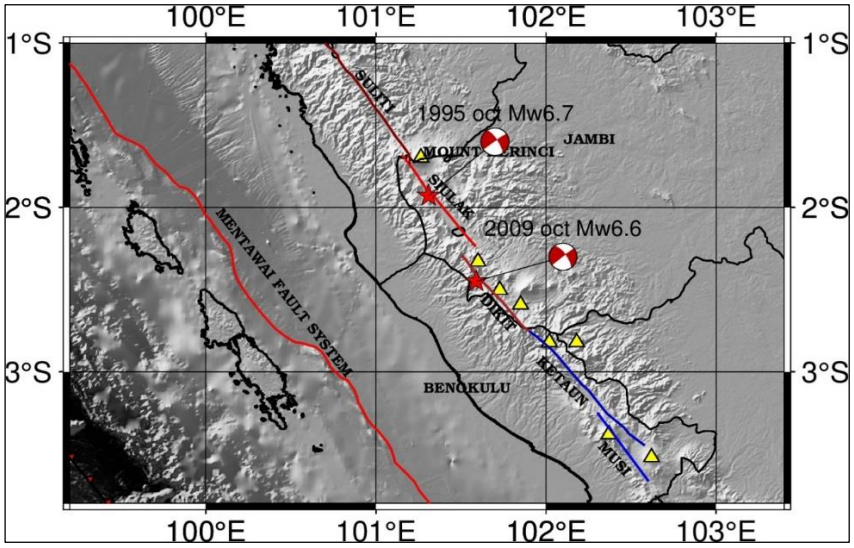

Fig. 3. Focal mechanism map of the 1995 Mw 6.7 Earthquake and the 2009 Mw 6.6 Earthquake with subduction earthquake.

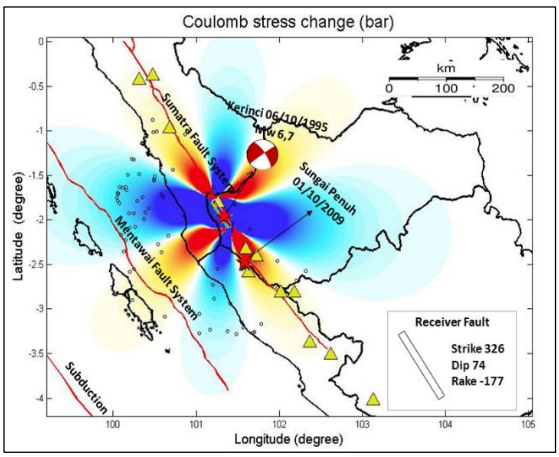

Fig. 4. Processing of coulomb stress of Kerinci earthquake 1995 Mw 6.7 from Global CMT with Nodal Plane 1 and seismicity distribution map after 1995 earthquake.

Based on Figure 4, it can be seen that the direction of the fault produced by the earthquake is parallel to the direction of the Sumatra Fault System. In this coulomb stress calculation, 2 lobes are produced, namely the red lobe and the blue lobe. The red lobe produces 4 directions, namely Northwest, Northeast, Southeast and Southwest of the epicenter. Meanwhile, the blue lobe also produces 4 directions, namely North, East, South and West of the epicenter. In addition, aftershocks obtained after the 1995 earthquake showed that many earthquakes occurred in the Mentawai Fault System area. The significant increase in seismicity was in the stress shadow area, which is in the West and North of the epicenter of the earthquake. Based on theory, this indicates that the increase in seismicity in the stress shadow area was not caused by the 1995 Mw 6.7 Kerinci earthquake. The increase in seismicity in the red lobe, namely in the Northwest, Southeast and Southwest directions from the epicenter, also experienced an increase in seismicity. However, in the Northeast direction, namely the direction of the Jambi Basin, there was no seismicity in the area (Asnawi et al., 2024, Simanjuntak et al., 2024). In addition, the Southwest direction did not experience a significant increase in seismicity as in other directions.

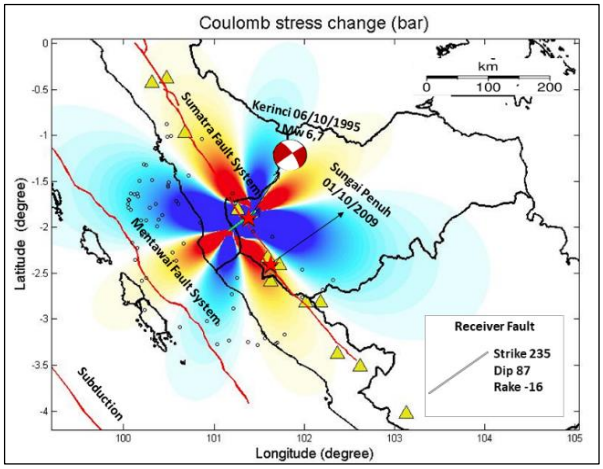

Fig. 5. Processing of coulomb stress of Kerinci earthquake 1995 Mw 6.7 from Global CMT with Nodal Plane 2 and seismicity distribution map after 1995 earthquake.

Besides that, the red lobe in the Southeast direction is the epicenter of the 2009 Mw 6.6 Sungai Penuh earthquake. This also applies to Nodal Plane 2 as shown in Figure 5.

Figure 5 shows us that the fault direction of the Kerinci earthquake using the 2nd nodal plane is perpendicular to the Sumatra Fault System. In addition, this difference causes differences in the value of coulomb stress. In Nodal Plane 1, the epicenter of this earthquake experienced a decrease in stress of 13,355 bar while in Nodal Plane 2 it also experienced a greater decrease in stress of 13,546 bar. However, the resulting lobes also point in the same direction as in Nodal Plane 1. The red lobes point to the Northwest, Northeast, Southeast and Southwest of the epicenter while the stress shadow points to the North, East, South and West of the epicenter. We calculated the coulomb stress for the 2009 Sungai Penuh Mw 6.6 earthquake also using 2 Nodal Planes. The calculation of Nodal Plane 1 can be seen in Figure 6.

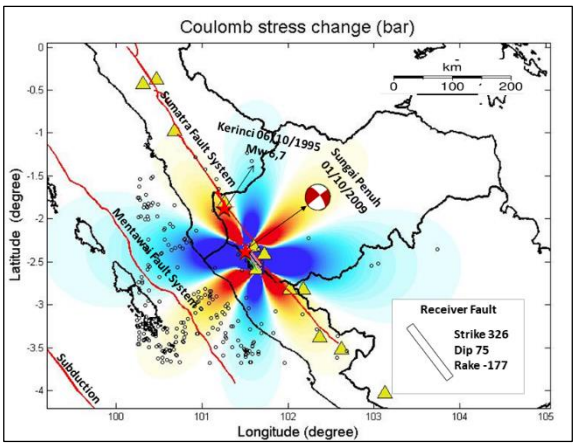

Fig. 6. Processing of coulomb stress of Sungai Penuh 2009 Mw 6.6 earthquake from Global CMT with Nodal Plane 1 and seismicity distribution map 2009 earthquake.

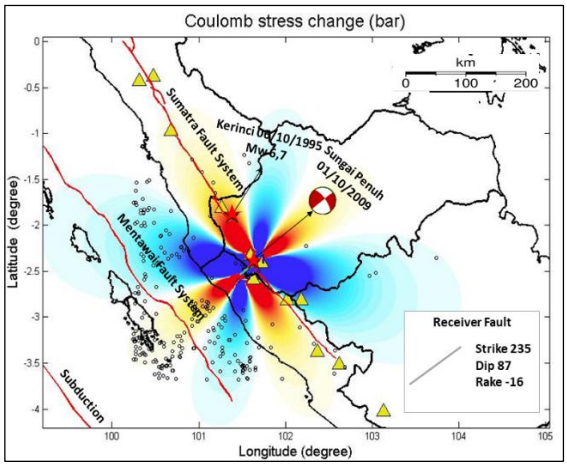

Fig. 7. Processing of coulomb stress of Sungai Penuh earthquake 1995 Mw 6.7 from Global CMT with Nodal Plane 2 and seismicity distribution map after 1995 earthquake.

Based on Figure 6, it can be seen that the fault direction of the 2009 Mw 6.6 Earthquake is parallel to the direction of the Sumatra Fault System. This coulomb stress calculation also produces 2 lobes, namely the red and blue lobes. The red lobe points to the northwest, northeast, southeast, and southwest of the epicenter. Meanwhile, the blue lobe points to the North, East, South and West of the epicenter. This is also exactly the same as the direction of the lobes in the 1995 Mw 6.7 Earthquake. In addition, seismicity after the 2009 earthquake was also spread over the study area.

The most significant increase occurred in the direction of the Mentawai Fault System, especially in the Southwest direction of the epicenter. In this area, there is very much earthquake activity after the 2009 earthquake. It also occurs in the stress shadow area. However, the increase in the stress shadow area means that the increase in seismicity in the area was not caused by the 2009 earthquake. Although the seismicity in the Mentawai Fault System area is very much, but in the Southeast and Northwest directions there is very little earthquake activity. We also calculated the coulomb stress of 2009 Sungai Penuh earthquake Mw 6.6 with Nodal Plane 2 as shown in Figure 7.

Based on Figure 7, as in Nodal Plane 2 of the 1995 Mw 6.7 Earthquake, the resulting fault direction is perpendicular to the direction of the Sumatra Fault System. This difference can also be seen in the calculation of coulomb stress. In Nodal Plane 1, the epicenter experienced a decrease in stress of 13.613 bar, while Nodal Plane 2 experienced a smaller decrease in stress of 13.289 bar. Similar to Nodal Plane 1, the direction of the red lobe produced by Nodal Plane 2 is towards the Northwest, Northeast, Southeast, and Southwest of the epicenter. While the stress shadow points to the North, East, South, West of the epicenter. Generally, the processing of the Coulomb stress of the Kerinci earthquake on October 6, 1995 Mw 6.7 and the Sungai Penuh earthquake on October 1, 2009 Mw 6.6, it can be seen that there are 2 lobe fields, namely the red lobe and the blue lobe. The red color lobe describes the area of increased coulomb stress while the blue color lobe describes the area of decreased coulomb stress or shadow stress. Measurements for the 1995 Mw 6.7 earthquake as shown in figures 4 & 5, The red lobe points to the Northwest (Suliti Segment), Northeast (Jambi Basin), Southeast (Dikit Segment), and Southwest (Mentawai Fault System) of the epicenter. The blue lobes point to the North, East, South, and West of the epicenter. Likewise, Nodal Plane 2 has the same lobe direction as Nodal Plane 1. However, the difference between these two Nodal Planes is that the direction of the fault on Nodal Plane 1 is parallel to the direction of the Sumatra Fault System, while the direction of the fault on Nodal Plane 2 is perpendicular to the direction of the Sumatra Fault System. Measurements for the 2009 Mw 6.6 earthquake as shown in Figure 6 & 7 have two lobe planes. The red-colored lobe plane points to the Northwest (Siulak Segment), Northeast (Jambi Basin), Southeast (Ketaun Segment), and Southwest (Mentawai Fault System) of the epicenter.

Based on 1995 Mw 6.7 Kerinci and 2009 Mw 6,6 earthquakes, after the earthquake occurred, Seismicity increase leads to Mentawai Fault System that happens in megathrust area. This was revealed by (Toda et al., 2005) that areas experiencing increased coulomb stress result in high seismicity. This is due to several factors, one of which is the background seismicity of the area. According (Hutchings & Mooney, 2021), The Mentawai Fault System area has high background seismicity and is dominated by shallow depth earthquakes. So, even the increase stress is low, the seismicity after earthquakes will be high in this area. Looking at the Southeast, Northwest and Northeast directions after the 1995 Mw 6.7 earthquake as shown in Figures 4 and 5, it can be seen that seismicity in these areas was, in general, slight.

In the southeast region of the Dikit Segment, which was the epicenter of the 2009 Mw 6.6 earthquake, seismicity

was low before the 2009 earthquake. We then calculated the increase in coulomb stress at the epicenter of the 2009 earthquake using equation 1. We found an increase of 7.9 kPa in Nodal plane 1 and 7.6 kPa in Nodal Plane 2. This was also mentioned by (Hurukawa et al., 2014; Natawidjaja & Triyoso, 2007) that the Dikit Segment area is one of the seismic gap areas. This explains that areas that experience decreased seismicity, or seismic quiescence, have the potential for earthquakes to occur (Wiemer & Wyss, 1994). In addition, the area that experienced an increase in coulomb stress but decreased seismicity was also in the northwest direction of the earthquake, namely the Suliti segment. This is also mentioned by research (Syafriani et al., 2020) which states that the Suliti Segment area has a low b-value which correlates with high stress conditions that have the potential for earthquakes. Similarly, the Ketaun Segment to the southeast of the 2009 Mw 6.6 earthquake, as shown in Figures 6 and 7, has low seismicity. This is also shown from research (Qiu & Chan, 2019, Nadia et al., 2023, Kuncoro et al., 2024) that the segments in Bengkulu Province experienced an increase in coulomb stress of more than 1 bar.

However, the low seismicity that occurs in onshore earthquakes, according to (Marsan, 2003), At high time scales static coulomb stress does not systematically control seismicity. This is evidenced by the fact that in the region of both the 1995 and 2009 earthquakes, the northeast, i.e. towards the Jambi Basin, has no seismicity at all. In fact, according to (Sari et al., 2023, Idha et al., 2023, Irwandi et al., 2021, Siringoringo et al., 2024) Back arc Basins of Jambi There is deformation so that there are several small segments that should be when the increase in coulomb stress in this direction also produces seismicity. Besides that, the southwest and northwest directions have high seismicity. This is in fact also influenced by the background seismicity of the area. According to (Ishibe et al., 2011) Estimating the background seismicity level is not straightforward due to the limited knowledge about small-magnitude earthquakes. Perhaps, the high seismicity in the blue lobe region could be caused by another mainshock. In addition, the use of the simple static stress change model also makes it difficult to explain the seismicity in the blue lobe region. According to (Felzer & Brodsky, 2005, Simanjuntak et al., 2018), static stress change does not affect seismicity after a mainshock.

There are several possible contributing factors to determine the seismicity behavior and potential occurrence of future large earthquakes. First, the determination of Magnitude of Completeness and Seismic Rate Change. Areas that have a small Magnitude of Completeness and have a high Seismic Rate Change can see better seismic activity so that they can see the correlation between static coulomb stress and seismicity (e.g. Ma et al., 2005). Second, the determination of the Receiver Fault. Based on our study, both receiver fault mechanisms produce large errors in the complex regional stress field. Third, Pore-fluid pressure. Many studies mention that a constant friction coefficient, such as μ'=0.4, can reduce the uncertainty of the measurement results. However, during a large earthquake, pore-fluid pressure changes significantly in the vicinity of the earthquake, so the use of a constant friction coefficient can cause significant errors in the estimation of stress change and seismic hazard (e.g. Beeler et al., 2000; Cocco & Rice, 2002).

4. Conclusion

This study aims to investigate the coulomb stress influence of Earthquakes Kerinci 1995 Mw 6.7 and Sungai Penuh 2009 Mw 6.6 on Seimicity Condition. In this study we use data form USGS with M ≥4. Both earthquakes have strike-slip type earthquakes. The seismicity condition correlates with ΔCFF in Mentawai Fault System. But it does not correlate in Suliti Segment, Ketaun Segment, and Back arc Basin of Jambi. Seismicity actually increases in the stress reduction area. This is caused by the influence of background seismicity so that the use of small magnitude catalog becomes important in the calculation analysis. Simplicity in calculation causes difficulty in explaining seismicity, especially in the blue lobe. Moreover, the use of receiver fault mechanism produces a very large error in the complex regional stress field. The use of a constant friction coefficient also produces a very large error in the calculation.

Acknowledgements

We thank to Meteorological Climatology and Geophysical Agency (BMKG) for providing the seismic data. We thank Global Centroid Moment Tensor (GCMT) for providing focal mechanism parameter. We thank for the fruitful discussion and comments from Editor and Reviewer.

References

Adi, S. P., Simanjuntak, A. V., Supendi, P., Wei, S., Muksin, U., Daryono, D., ... & Sinambela, M. (2024). Different Faulting of the 2023 (Mw 5.7 and 5.9) South-Central Java Earthquakes in the Backthrust Fault System. *Geotechnical and Geological Engineering*, 1-13.

Andinisari, R., Simanjuntak, A. V., & Dhanarsari, R. A. (2024, July). Absolute locations of earthquakes in eastern java determined by using a minimum 1D P-wave velocity model. In AIP Conference Proceedings (Vol. 3077, No. 1). AIP Publishing.

Ansari, K., Walo, J., Simanjuntak, A. V., & Wezka, K. (2024). Crustal deformation from GNSS measurement and earthquake mechanism along Pieniny Klippen Belt, Southern Poland. *Arabian Journal of Geosciences*, *17*(6), 180.

Ansari, K., Walo, J., Simanjuntak, A. V., & Wezka, K. (2024). Evaluation of recent Tectonic movement in Northeast Japan by using long-term GNSS and Tide Gauge Measurements. Journal of Structural Geology, 105258.

Asnawi, Y., Gunaya, M., Prayitno, S., Simanjuntak, A., & Muksin, U. (2024). Simulation Of Earthquake Intensity For Tsunami Prediction And Disaster Risk Management. *GEOMATE Journal*, *26*(118), 17-24.

Asnawi, Y., Simanjuntak, A. V., Umar, M., Rizal, S., & Syukri, M. (2020). A microtremor survey to identify seismic vulnerability around Banda Aceh using HVSr analysis. *Elkawnie: Journal of Islamic Science and Technology*, *6*(2), 342-358.

Asnawi, Y., Simanjuntak, A., Muksin, U., Rizal, S., Syukri, M. S. M., Maisura, M., & Rahmati, R. (2022). Analysis of microtremor H/V spectral ratio and public perception for disaster mitigation. *GEOMATE Journal*, *23*(97), 123-130.

Beeler, N. M., Simpson, R. W., Hickman, S. H., & Lockner, D. A. (2000). Pore fluid pressure, apparent friction, and Coulomb failure. *Journal of Geophysical Research: Solid Earth*, *105*(B11), 25533–25542. https://doi.org/10.1029/2000jb900119

Bellier, O., Sébrier, M., Pramumijoyo, S., Beaudouin, T.,

Harjono, H., Bahar, I., & Forni, O. (1997). Paleoseismicity and seismic hazard along the Great Sumatran fault (Indonesia). *Journal of Geodynamics*, *24*(1–4), 169–183. https://doi.org/10.1016/s0264-3707(96)00051-8

Charles, G., King, P., & Lin, J. (1994). Static Stress Changes and the Triggering of Earthquakes. *Bulletin of the Seismological Society of America*, *84*, 935–953. https://www.researchgate.net/publication/237500715

Cocco, M., & Rice, J. R. (2002). Pore pressure and poroelasticity effects in Coulomb stress analysis of earthquake interactions. *Journal of Geophysical Research: Solid Earth*, *107*(B2). https://doi.org/10.1029/2000jb000138

DeMets, C., Gordon, R. G., & Argus, D. F. (2010). Geologically current plate motions. *Geophysical Journal International*, *181*(1), 1–80. https://doi.org/10.1111/j.1365-246X.2009.04491.x

Felzer, K. R., & Brodsky, E. E. (2005). Testing the stress shadow hypothesis. *Journal of Geophysical Research: Solid Earth*, *110*(5), 1–13. https://doi.org/10.1029/2004JB003277

Genrich, J. F., Bock, Y., McCaffrey, R., Prawirodirdjo, L., Stevens, C. W., Puntodewo, S. S. O., Subarya, C., & Wdowinski, S. (2000). Distribution of slip at the northern Sumatran fault system. *Journal of Geophysical Research: Solid Earth*, *105*(B12), 28327–28341. https://doi.org/10.1029/2000jb900158

Harris, R. A., & Simpson, R. W. (1996). In the shadow of 1857-the effect of the great Ft. Tejon earthquake on subsequent earthquakes in southern California. *Geophysical Research Letters*, *23*(3), 229–232.

Hurukawa, N., Wulandari, B. R., & Kasahara, M. (2014). Earthquake history of the Sumatran fault, Indonesia, since 1892, derived from relocation of large earthquakes. *Bulletin of the Seismological Society of America*, *104*(4), 1750–1762. https://doi.org/10.1785/0120130201

Hutchings, S. J., & Mooney, W. D. (2021). The Seismicity of Indonesia and Tectonic Implications. *Geochemistry, Geophysics, Geosystems*, *22*(9). https://doi.org/10.1029/2021GC009812

Idha, R., Sari, E. P., Asnawi, Y., Simanjuntak, A. V., Humaidi, S., & Muksin, U. (2023). 1-Dimensional Model of Seismic Velocity after Tarutung Earthquake 1 October 2022 Mw 5.8. *Journal of Applied Geospatial Information*, *7*(1), 825-831.

Idha, R., Sari, E. P., Humaidi, S., Simanjuntak, A. V., & Muksin, U. (2023, December). Response of Geologic Units to The Ground Parameters of Tarutung Earthquake 2022 Mw 5.8: A Preliminary Study. In *IOP Conference Series: Earth and Environmental Science* (Vol. 1288, No. 1, p. 012032). IOP Publishing.

Irwandi, I., Muksin, U., & Simanjuntak, A. V. (2021). Probabilistic seismic hazard map analysis for Aceh Tenggara district and microzonation for Kutacane city. In *IOP Conference Series: Earth and Environmental Science* (Vol. 630, No. 1, p. 012001). IOP Publishing.

Ishibe, T., Shimazaki, K., Tsuruoka, H., Yamanaka, Y., & Satake, K. (2011). Correlation between Coulomb stress changes imparted by large historical strike-slip earthquakes and current seismicity in Japan. *Earth, Planets and Space*, *63*(3), 301–314. https://doi.org/10.5047/eps.2011.01.008

Kilb, D., Gomberg, J., & Bodin, P. (2002). Aftershock triggering by complete Coulomb stress changes. *Journal of Geophysical Research: Solid Earth*, *107*(B4). https://doi.org/10.1029/2001jb000202

Kuncoro, D., Asnawi, Y., Halauwet, Y., Simanjuntak, A., & Susilo, A. (2024). SEISMOTECTONIC ANALYSIS OF MW 7.6 2023 SOUTH MOLUCCA INTERMEDIATE-DEPTH EARTHQUAKE. *GEOMATE Journal*, *27*(120), 9-16.

Lin, J., & Stein, R. S. (2004). Stress triggering in thrust and subduction earthquakes and stress interaction between the southern San Andreas and nearby thrust and strike-slip faults. *Journal of Geophysical Research: Solid Earth*, *109*(B2). https://doi.org/10.1029/2003jb002607

Ma, K. F., Chan, C. H., & Stein, R. S. (2005). Response of seismicity to Coulomb stress triggers and shadows of the 1999 Mw=7.6 Chi-Chi, Taiwan, earthquake. *Journal of Geophysical Research: Solid Earth*, *110*(5), 1–16. https://doi.org/10.1029/2004JB003389

Marsan, D. (2003). Triggering of seismicity at short timescales following Californian earthquakes. *Journal of Geophysical Research: Solid Earth*, *108*(B5). https://doi.org/10.1029/2002jb001946

Nadia, M., Simanjuntak, A. V., Arifullah, A., Sugiyanto, D., & Muksin, U. (2023, December). Preliminary Result of Swarm Activities in Toba Region Using Dense Temporary Network. In *IOP Conference Series: Earth and Environmental Science* (Vol. 1288, No. 1, p. 012025). IOP Publishing.

Natawidjaja, D. H. (2018). Updating active fault maps and sliprates along the Sumatran Fault Zone, Indonesia. *IOP Conference Series: Earth and Environmental Science*, *118*(1), 1–11. https://doi.org/10.1088/1755-1315/118/1/012001

Natawidjaja, D. H., & Triyoso, W. (2007). The Sumatran Fault Zone-from Source to Hazard. *Journal of Earthquake and Tsunami*, *1*(1), 21–47.

Nurana, I., Simanjuntak, A. V., Umar, M., Kuncoro, D. C., Syamsidik, S., & Asnawi, Y. (2021). Spatial Temporal Condition of Recent Seismicity In The Northern Part of Sumatra. *Elkawnie: Journal of Islamic Science and Technology*, *7*(1), 131-145.

Okada, Y. (1992). Internal Deformation due to Shear and Tensile Faults in a Half-Space. In *Bulletin of the Seismological Society of America* (Vol. 82, Issue 2).

Parsons, T., & Dreger, D. S. (2000). Static-stress impact of the 1992 Landers earthquake sequence on nucleation and slip at the site of the 1999 M=7.1 Hector Mine earthquake, southern California. *Geophysical Research Letters*, *27*(13), 1949–1952. https://doi.org/10.1029/1999GL011272

Pasari, S., Simanjuntak, A. V., Neha, & Sharma, Y. (2021). Nowcasting earthquakes in Sulawesi island, Indonesia. *Geoscience Letters*, *8*, 1-13.

Pasari, Sumanta, Andrean VH Simanjuntak, Anand Mehta, Neha, and Yogendra Sharma. "A synoptic view of the natural time distribution and contemporary earthquake hazards in Sumatra, Indonesia." *Natural Hazards* 108 (2021): 309-321.

Qadariah, Q., Simanjuntak, A. V., & Umar, M. (2018). Analysis of Focal Mechanisms Using Waveform Inversion; Case Study of Pidie Jaya Earthquake December 7, 2016. *Journal of Aceh Physics Society*, *7*(3), 127-132.

Qiu, Q., & Chan, C. H. (2019). Coulomb stress perturbation after great earthquakes in the Sumatran subduction zone: Potential impacts in the surrounding region.

Journal of Asian Earth Sciences, *180*. https://doi.org/10.1016/j.jseaes.2019.103869

Salman, R., Lindsey, E. O., Feng, L., Bradley, K., Wei, S., Wang, T., Daryono, M. R., & Hill, E. M. (2020). Structural Controls on Rupture Extent of Recent Sumatran Fault Zone Earthquakes, Indonesia. *Journal of Geophysical Research: Solid Earth*, *125*(2). https://doi.org/10.1029/2019JB018101

Sari, E. P., Idha, R., Asnawi, Y., Simanjuntak, A., Humaidi, S., & Muksin, U. (2023). Faulting Mechanism of Tarutung Earthquake 2022 Mw 5.8 Using Moment Tensor Inversion. *Journal of Applied Geospatial Information*, *7*(1), 840-846.

Sieh, K., & Natawidjaja, D. (2000). Neotectonics of the Sumatran fault, Indonesia. *Journal of Geophysical Research: Solid Earth*, *105*(B12), 28295–28326. https://doi.org/10.1029/2000jb900120

Simanjuntak, A. V., & Ansari, K. (2022). Seismicity clustering of sequence phenomena in the active tectonic system of backthrust Lombok preceding the sequence 2018 earthquakes. *Arabian Journal of Geosciences*, *15*(23), 1730.

Simanjuntak, A. V., & Ansari, K. (2023). Spatial time cluster analysis and earthquake mechanism for unknown active fault (Kalatoa fault) in the Flores Sea. *Earth Science Informatics*, *16*(3), 2649-2659.

Simanjuntak, A. V., & Ansari, K. (2024). Multivariate hypocenter clustering and source mechanism of 2017 Mw 6.2 and 2019 Mw 6.5 in the South Seram subduction system. *Geotechnical and Geological Engineering*, 1-14.

Simanjuntak, A. V., & Olymphia, O. (2017). Perbandingan Energi Gempa Bumi Utama dan Susulan (Studi Kasus: Gempa Subduksi Pulau Sumatera dan Jawa). *Jurnal Fisika Flux: Jurnal Ilmiah Fisika FMIPA Universitas Lambung Mangkurat*, *14*(1), 19-26.

Simanjuntak, A. V., Muksin, U., & Sipayung, R. M. (2018, December). Earthquake relocation using HypoDDMethod to investigate active fault system in Southeast Aceh. In *Journal of Physics: Conference Series* (Vol. 1116, No. 3, p. 032033). IOP Publishing.

Simanjuntak, A. V., Palgunadi, K. H., Supendi, P., Muksin, U., Gunawan, E., Widiyantoro, S., ... & Ida, R. (2024). The western extension of the Balantak Fault revealed by the 2021 earthquake cascade in the central arm of Sulawesi, Indonesia. *Geoscience Letters*, *11*(1), 35.

Siringoringo, L. P., Sapiie, B., Rudyawan, A., & Sucipta, I. G. B. E. (2024). Origin of high heat flow in the back-arc basins of Sumatra: An opportunity for geothermal energy development. *Energy Geoscience*, *5*(3). https://doi.org/10.1016/j.engeos.2024.100289

Stein, R. S., King, G. C. P., & Lin, J. (1992). Change in failure stress on the southern San Andreas fault system caused by the 1992 magnitude = 7.4 Landers earthquake. *Science*, *258*(5086), 1328–1332. https://doi.org/10.1126/science.258.5086.1328

Stein, R. S., King, G. C. P., & Lin, J. (1994). Stress triggering of the 1994 M = 6.7 Northridge, California, Earthquake by its predecessors. *Science*, *265*(5177), 1432–1435. https://doi.org/10.1126/science.265.5177.1432

Syafriani, S., Raeis, M., & Hamdi. (2020). Local stress and seismic activity at West Sumatra. *Journal of Physics: Conference Series*, *1481*(1). https://doi.org/10.1088/1742-6596/1481/1/012002

Toda, S. (2008). Coulomb stresses imparted by the 25 March 2007 Mw=6.6 Noto-Hanto, Japan, earthquake explain its 'butterfly' distribution of aftershocks, and suggest a heightened seismic hazard. *Earth Planets Space*, *60*, 1041–1046.

Toda, S., & Stein, R. S. (2002). Response of the San Andreas fault to the 1983 Coalinga-Nuñez earthquakes: An application of interaction-based probabilities for Parkfield. *Journal of Geophysical Research: Solid Earth*, *107*(B6). https://doi.org/10.1029/2001jb000172

Toda, S., Stein, R. S., Reasenberg, P. A., Dieterich, J. H., & Yoshida, A. (1998). Stress transferred by the 1995 Mw = 6.9 Kobe, Japan, shock: Effect on aftershocks and future earthquake probabilities. *Journal of Geophysical Research: Solid Earth*, *103*(10), 24543–24565. https://doi.org/10.1029/98jb00765

Toda, S., Stein, R. S., Richards-Dinger, K., & Bozkurt, S. B. (2005). Forecasting the evolution of seismicity in southern California: Animations built on earthquake stress transfer. *Journal of Geophysical Research: Solid Earth*, *110*(5), 1–17. https://doi.org/10.1029/2004JB003415

Weller, O., Lange, D., Tilmann, F., Natawidjaja, D., Rietbrock, A., Collings, R., & Gregory, L. (2012). The structure of the Sumatran Fault revealed by local seismicity. *Geophysical Research Letters*, *39*(1). https://doi.org/10.1029/2011GL050440

Wells, D. L., & Coppersmith, K. J. (1994). New Empirical Relationships among Magnitude, Rupture Length, Rupture Width, Rupture Area, and Surface Displacement. *Bulletin of the Seismological Society of America*, *84*(4), 974–1002.

Wiemer, S., & Wyss, M. (1994). Seismic Quiescence before the Landers (M = 7.5) and Big Bear (M = 6.5) 1992 Earthquakes. In *Bulletin of the Seismological Society of America* (Vol. 84, Issue 3).

Woessner, J., Jónsson, S., Sudhaus, H., & Baumann, C. (2012). Reliability of Coulomb stress changes inferred from correlated uncertainties of finite-fault source models. *Journal of Geophysical Research: Solid Earth*, *117*(7). https://doi.org/10.1029/2011JB009121